DIRECT DETERMINATION OF THE LAMELLAR STRUCTURE OF PERIPHERAL NERVE MYELIN AT LOW RESOLUTION (17 Å)

T. J. McINTOSH *and* C. R. WORTHINGTON

From the Departments of Biological Sciences and Physics, Carnegie-Mellon University, Pittsburgh, Pennsylvania 15213

ABSTRACT New X-ray diffraction data from normal nerve and nerve swollen in glycerol solutions have been recorded. Direct methods of structure analysis have been used in the interpretation of the X-ray data, and the phases of the first five orders of diffraction of peripheral nerve myelin have been uniquely determined. The direct methods include deconvolution of the autocorrelation function, sampling theorem reconstructions, and Fourier synthesis comparisons. Electron density profiles of normal and swollen nerve myelin at a resolution of 17 Å together with an electron density scale in electrons per cubic angstrom are presented.

INTRODUCTION

The molecular structure of nerve myelin occupies a special place in our knowledge of the structure and function of biological membranes. It was recognized early in the 20th century that nerve myelin had a high degree of molecular order and was therefore suitable for study by diffraction and microscopy. Although X-ray diffraction patterns were recorded in the early 1930's, it is only in recent years that information on the nerve myelin structure has been obtained.

Nerve myelin refers to the sheath of lipoprotein which surrounds the axon of myelinated nerve at periodic intervals along its length. The myelin sheath of peripheral nerve is derived from a spiral wrapping of Schwann's cell membranes around the axon (Geren, 1954). This mode of formation means that the unit cell is centrosymmetrical and contains two membranes. These two membranes come together during myelination to form the membrane pair.

Nerve myelin has been extensively studied by diffraction and microscopy. An account of the early history of structural studies can be found in recent reviews (Finean, 1969; Worthington, 1971; Worthington, 1973 *a*). The interpretation of the low-angle X-ray diffraction intensities from nerve leads to a description of the one-dimensional electron density distribution at right angles to the surface of the myelin sheath. The resolution Δx of a Fourier series representation of this electron density

is given by $\Delta x = d(2h)^{-1}$ where d is the radial repeat distance and h is the number of diffraction orders used in the synthesis. The 1941 low-angle X-ray diffraction pattern from frog sciatic nerve (Schmitt et al., 1941) had $d = 171$ Å, $h = 5$, and hence, Δx of the Fourier synthesis is 17 Å. This resolution of 17 Å is called low resolution as higher orders of diffraction have been recorded (Blaurock and Worthington, 1969) and resolution considerably better than 17 Å is possible.

The lamellar structure at low resolution is obtained as a result of computing the appropriate Fourier series representation for nerve. This means that the correct Fourier coefficients and the correct phases associated with the Fourier coefficients have to be found. The first problem has been solved, that is, the Fourier coefficients can be obtained from the intensities of the X-ray reflections after suitable processing (Blaurock and Worthington, 1966). The problem of finding the first five phases is considered in this paper. Fortunately, the phases can only be + or − as the unit cell is centrosymmetrical. Thus, there are only 2^5 or 32 different ways of assigning phases to the first five diffraction orders of nerve. The essential difficulty with choosing the correct set of phases is that there is no way of deciding which profile of the 32 possible Fourier profiles might be the correct one solely on the basis of the X-ray data from live nerve. A particular profile can, of course, be derived on the basis of certain assumptions, but the correct structure is sought and this means that a proof of correctness is needed.

Progress towards finding the correct set of phases depends on obtaining additional information. This additional information has been obtained as a result of swelling experiments. This property of swelling (or shrinking) is important for it suggests the possibility of deducing the shape of the Fourier transform, a method which was first used with hemoglobin crystals by Boyes-Watson and Perutz (1943). Nerve myelin is known to swell in hypotonic solutions (Finean and Millington, 1957) and this swelling occurs between adjacent membrane pairs (Robertson, 1958). In the early 1960's, X-ray diffraction patterns were recorded from swollen nerve but the structure analyses of these patterns were not complete (Finean and Burge, 1963; Moody, 1963). Finean and Burge (1963) assigned phases on the assumption that the principle of minimum wavelength (Perutz, 1954) applied to the nerve data. However, in later work on hemoglobin crystals (Perutz, 1954) it was found that this principle was not rigorously obeyed so that a more reliable method of phase determination is needed. It is interesting to note that in recent X-ray studies on membranes, the Fourier transforms of retinal photoreceptors (Worthington, 1973 *b*), sarcoplasmic reticulum membranes (Worthington and Liu, 1973) and a calculated bilayer model (see Fig. 9 of Worthington [1973 *a*]) all show deviations from this principle of minimum wavelength. Moody (1963) avoided these pitfalls and used the sampling theorem of communication theory (Shannon, 1949) to deduce a set of phases for nerve. But Moody (1963) was unable to decide between two possible phase choices (−, +, +, −, −) and (−, +, +, +, +) for the $h = 5$ orders of nerve. Finean and Burge (1963) proposed the phases (−, +, +, −,−) and noted

that this phase choice gave rise to a bilayer profile. However, definitive evidence for this conclusion had not been obtained and, moreover, the Fourier profiles of Finean and Burge (1963) were incorrect in detail for incorrect Fourier coefficients had been used (Blaurock and Worthington, 1966).

Improved X-ray diffraction patterns of frog sciatic nerve swollen in sucrose solutions were recorded by Worthington and Blaurock (1969 *a*) and the structure analysis of the X-ray data from swollen and normal nerve strongly supported the phase choice (−, +, +, −, −) for the $h = 5$ orders of normal nerve (Worthington and Blaurock, 1969 *b*). The 1969 structure analysis (Worthington and Blaurock, 1969 *b*) had the advantage of using new X-ray data from swollen nerve and using new methods of X-ray analysis and it did seem as if the low-resolution structure of nerve had been solved. But a proof of correctness was not obtained and, moreover, many people questioned the swelling experiments as sucrose solutions can pass through a variety of membranes. These questions were not easily answered although it was shown that the swelling of frog sciatic nerve in distilled water was reversible (Worthington and Blaurock, 1969 *a*). Complications, however, arose when it was argued that the phases of swollen nerve also applied to normal nerve. The difficulty was that the membrane pair of swollen nerve did not have the same structure as the membrane pair of normal nerve. This change in membrane pair structure on swelling was later shown to be due to a change in the width of the cytoplasmic fluid layer at the center of the membrane pair with the single membrane structure remaining uneffected (Worthington, 1969 *a*). In retrospect, the sucrose data, although the best available, did have limitations. The electron density profiles of the nerve myelin membrane in different sucrose concentrations did not superimpose; the central narrow low density region tends to be wider as the sucrose concentration is increased (Worthington and Blaurock, 1969 *b*). Thus, it was evident that, in order to more firmly establish the correctness of the low-resolution structure of nerve, even better swelling data than the sucrose data were needed.

In the early 1970's, two other solutions to the phase problem of nerve were presented (Akers and Parsons, 1970; Harker, 1972). Akers and Parsons (1970) from a study of nerve, chemically treated with heavy atoms, deduced the phase choice (+, +, +, +, +) for the $h = 5$ orders of nerve. However, this analysis was shown to be in error (Worthington, 1970) and, moreover, it was shown that the Akers and Parsons (1970) data did not conflict with the (−, +, +, −, −) phase choice obtained by Worthington and Blaurock (1969 *a*). Harker (1972) in an independent analysis of the Akers and Parsons (1970) data obtained two sets of phases (+, −, −, +, +) and (−, +, +, −, −) for nerve. These two phase choices are referred to as the negative and positive structures, respectively. Harker (1972) preferred the negative structure but a choice between the two structures has been made in favour of the positive structure (McIntosh and Worthington, 1973). Thus, even though evidence can be put forward which is in support of the phase choice (−, +, +, −, −), a proof of correctness had not been obtained in studies prior to 1973.

Improved low-angle X-ray diffraction patterns of frog sciatic nerve swollen in glycerol solutions have now been obtained. Higher-order diffraction from swollen nerve has been recorded so that the phases of the higher orders of normal nerve can be studied. An account of this moderate resolution study will be presented in a subsequent paper but a brief report of this work has already appeared (Worthington and McIntosh, 1973). The glycerol data can be used to directly determine the lamellar structure of nerve myelin at low resolution. The use of direct methods of structure analysis (Worthington et al., 1973) enables a proof of correctness to be given for the first time. Fortunately, the X-ray diffraction patterns of frog sciatic nerve swollen in glycerol solutions indicate that the membrane pair structure did not change on swelling. That is, the earlier complications with the sucrose data do not apply to the glycerol data. The structure analysis is therefore straightforward. Other X-ray diffraction experiments using glycerol and Ringer's solution are also described and these experiments provide verification that the correct choice of phases has been obtained. Moreover, the interpretation of new data from nerve swollen in glycerol solutions contributes towards an understanding of the swelling behavior of the nerve myelin sheath.

METHODS

Low-angle X-ray diffraction patterns were obtained from frog (*Rana pipiens*) sciatic nerve. Freshly dissected nerves were immersed in frog Ringer's solutions at room temperatures. Each nerve specimen, together with excess solution, was sealed in a thin-walled (10 μm thick) glass capillary tube. Nerves were swollen in glycerol solutions maintained at room temperatures and were sealed in capillary tubes similar to the fresh specimens.

Low-angle X-ray diffraction patterns were obtained using an optically focusing X-ray camera and an Elliott rotating anode micro-focus X-ray generator. The optically focusing X-ray camera was a modified version of an earlier design (Elliott and Worthington, 1963). Most patterns were recorded using slit collimation. Slit collimation was obtained using only the first mirror (horizontal) and a line focus (horizontal) on the copper anode.

The X-ray patterns were taken with nickel-filtered copper Kα radiation. The specimen-to-film distance was normally set at about 8.0 cm although it could be increased when required. Exposure times usually did not exceed 6 h. Note that in an early study (Blaurock and Worthington, 1969) it was demonstrated that the nerve myelin diffraction pattern did not change in any way for a period of about 1 day.

X-ray patterns were recorded on Ilford Industrial G film (Ilford Ltd., Ilford, Essex, England). Three films were placed in the cassette in order to give an adequate range of intensities. An intensity range of 300:1 was covered. Densitometer tracings of the X-ray patterns were obtained on a Joyce-Loebl microdensitometer model MK III C (Joyce-Loebl & Co., Burlington, Mass.) The background scattering curve was subtracted from the densitometer tracing in the usual way. The integrated intensities, $I(h)$ where h is the diffraction order, were measured by integrating the areas under the diffraction peaks.

DIFFRACTION THEORY

The structure analysis of the low-angle X-ray diffraction data from nerve myelin as used in this paper makes use of direct methods. These direct methods are based on

obtaining experimental data points which all lie on a continuous curve. Thus, the direct methods referred to in this paper are not the same as the direct methods of X-ray crystallography which refer to either finding relations between structure factors or refer to finding ways of directly interpreting the Patterson function. The direct methods in this paper are deconvolution and reconstruction methods. The deconvolution methods are based upon the original theory of Hosemann and Bagchi (1962) while the reconstruction methods are based on the sampling theorem of communication theory (Shannon, 1949) and on the usual Fourier series expressions. The diffraction theory has been given elsewhere (Worthington, 1969 *b*; Worthington, 1971, King and Worthington, 1971; Worthington et al., 1973) and only a brief account is given here. An attempt is made to retain the previous notation where possible.

Let $t(x)$ represent the electron density distribution in the radial direction of a single unit cell and let $T(X)$ represent its Fourier transform. Denote $t(x) \rightleftarrows T(X)$ where $t(x)$ and $T(X)$ are a pair of Fourier transforms, and where x, X are real and reciprocal space coordinates (Worthington, 1969 *b*). Nerve myelin has a multilayered assembly so that discrete reflections are recorded at $X = h/d$, h an integer. Integrated intensities $I(h)$ are measured from the X-ray film. Corrected intensities $J_{obs}(h)$ are, however, needed for the X-ray analysis and, according to Blaurock and Worthinton (1966), $J_{obs}(h) = hI(h)$. The notation $J(h) = |T(h)|^2$ and $KJ_{obs}(h) = J(h)$ is retained where K is the normalization constant. Thus, a set of corrected intensities $J_{obs}(h)$ is obtained from a diffraction experiment.

It is convenient to assume $K = 1$ and use $J(h)$ for the corrected intensities. This means that an interpretation of $t(x)$ on a relative scale is first sought. When the absolute scale is considered, then a precise value is assigned to K. Any two sets of low-angle X-ray data with different radial repeat distances d_1 and d_2 are placed on the same relative scale using the formula of Worthington and Blaurock (1969 *b*).

A model for $t(x)$ is considered which contains an extracellular fluid space. Let the membrane pair have electron density $m(x)$ and the fluid layer have electron density F. A drawing of this model can be found in Worthington et al., (1973) (see Fig. 3, p. 486). The membrane pair has average electron density M and width v and the fluid layer has width $d - v$. The origin of the unit cell is at the center of the membrane pair. It is, however, convenient to study the minus fluid model and this model is denoted $\Delta t(x)$ where $\Delta t(x) = t(x) - F$. A drawing of this model can be found in Worthington et al. (1973) (see Fig. 4, p. 486). The membrane pair has electron density $m(x) - F$ and the space $d - v$ has zero density.

The Fourier transform of $\Delta t(x)$ is $\Delta T(X)$ where $\Delta t(x) \rightleftarrows \Delta T(X)$. The relation between $T(X)$ and $\Delta T(X)$ is

$$\Delta T(X) = T(X) - Fd \operatorname{sinc} \pi dX, \tag{1}$$

where $\operatorname{sinc} \theta = \sin \theta/\theta$. Hence $\Delta T(h) = T(h)$ provided h is a non-zero integer.

This means that the two models cannot be distinguished on the basis of the low-angle X-ray data as the $h = 0$ reflection is not observed. The appropriate Fourier series representation for both models is

$$2/d \sum_{1}^{h} \{\pm\} \mid T(h) \mid \cos 2\pi hx/d, \tag{2}$$

where $\{\pm\}$ is the phase information. The appropriate Patterson function for both models is

$$2/d \sum_{1}^{h} J(h) \cos 2\pi hx/d. \tag{3}$$

The additional information is obtained from swelling experiments. The Fourier transform $\Delta T(X)$ for the minus fluid model is given by

$$\Delta T(X) = M(X) - Fv \operatorname{sinc} \pi vX, \tag{4}$$

where $M(X)$ is the Fourier transform of $m(x)$, i.e., $m(x) \rightleftarrows M(X)$. Discrete X-ray reflections occur at $X = h/d$, h an integer. If, by changing the immersion fluid and retaining the same electron density value F the unit cell size increases from d to D but with no change in $m(x)$ (which also implies no change in v), then the Fourier transform of the swollen minus fluid model is given by Eq. 4. Discrete X-ray reflections occur at $X = H/D$, H an integer. Thus, two sets of data $\Delta J(h)$ and $\Delta J(H)$ lie on the same intensity transform $\Delta J(X)$. A series of swelling experiments using the same F generally gives different repeat periods (Worthington and Blaurock, 1969 *a*). Thus, swelling experiments using the same fluid electron density F can provide many sampling points on $\Delta J(X)$. Knowledge of $\Delta J(X)$ is therefore obtained as a result of swelling experiments.

Direct methods of structure analysis can be used to derive the correct structure once knowledge of $\Delta J(X)$ is obtained. The theory of these direct methods as applied to multilayered membrane systems which contain fluid layers has been presented (Worthington et al., 1973). The direct methods use either deconvolution of the autocorrelation function or reconstruction methods. The deconvolution is performed using the relaxation method and the reconstruction methods use the sampling theorem series expressions to compute the continuous Fourier transform and use the Fourier series representation of Eq. 2 to compute the electron density.

RESULTS

Low-angle X-ray diffraction data from frog sciatic nerve swollen in glycerol solutions have been recorded. A series of X-ray experiments were performed using 0, 6.5, 15, and 50% glycerol while some experiments were also performed using 5, 10, 20, 30,

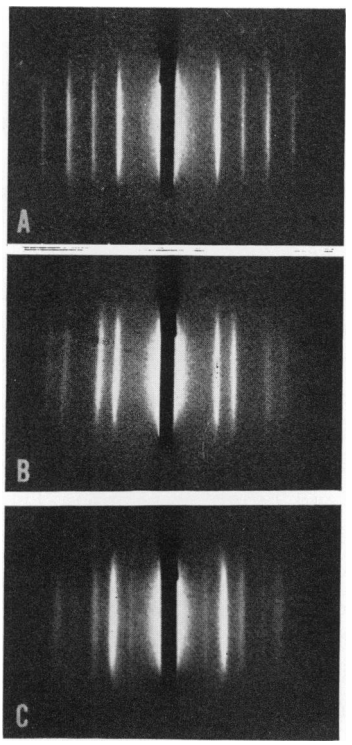

FIGURE 1

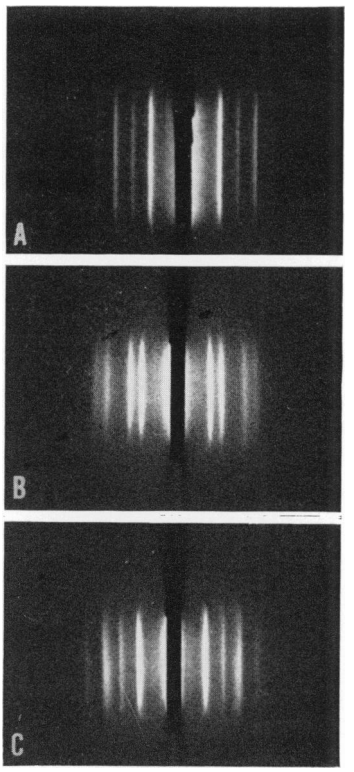

FIGURE 2

FIGURE 1 (*A*) Low-angle X-ray diffraction pattern of normal frog sciatic nerve myelin in Ringer's solution, d = 171 Å. The first five orders of diffraction are visible in the original negative. Scattering close to the beam stop partially obscures the first order in this reproduction. (*B*) Low-angle X-ray diffraction pattern of frog sciatic nerve myelin swollen in 6.5% glycerol, d = 250 Å. Orders h = 1, 3, 4, 6 and 7 are visible in this reproduction. The first eight orders are visible in the original negative. (*C*) Low-angle X-ray diffraction pattern of frog sciatic nerve myelin swollen in 6.5% glycerol, d = 226 Å. Orders h = 2, 3, 4, 5 and 6 are visible in this reproduction. The first seven orders are visible in the original negative.

FIGURE 2 (*A*) Low-angle X-ray diffraction pattern of normal frog sciatic nerve myelin in Ringer's solution, d = 171 Å. The first five orders of diffraction are visible. (*B*) Low-angle X-ray diffraction pattern of frog sciatic nerve myelin swollen in 5% glycerol, d = 247 A. Orders h = 1, 3, 4, 6 and 7 are visible in this reproduction. The first eight orders are visible in the original negative. (*C*) Low-angle X-ray diffraction pattern of myelin swollen in 5% glycerol (Fig. 2 *B*) and then reimmersed in Ringer's solution. The first five diffraction orders of the normal 171 Å repeat period are visible.

35, and 40% glycerol. In particular, many experiments were run using 6.5% glycerol as 6.5% glycerol has the same electron density as Ringer's solution.

Typical diffraction patterns of normal and swollen nerve in 6.5% glycerol are shown in Figs. 1 *A*, *B*, and *C*. The normal pattern from frog sciatic nerve in Ringer's solution has d = 171 Å and h = 5 orders and is shown in Fig. 1 *A*. Two swollen pat-

terns from frog sciatic nerve in 6.5% glycerol solution have d = 250 Å and d = 226 Å and are shown in Figs. 1 *B* and 1 *C*, respectively. All three X-ray patterns have minimum spacings of about 34 Å. The X-ray reflections in all three patterns are discrete and well separated so that the intensities have been accurately measured. The X-ray reflections in the normal pattern are very sharp as the myelin layers have precise order as noted previously (Blaurock and Worthington, 1969).

A series of experiments have been conducted to determine whether the swelling process is reversible. A diffraction pattern was recorded from nerve swollen in glycerol solution. The swollen nerve was then placed in Ringer's solution for several hours and another diffraction pattern was recorded. Typical diffraction patterns of normal, swollen nerve in 5% glycerol and the same swollen nerve rewet in Ringer's solution are shown in Figs. 2 *A*, *B*, and *C*, respectively. All three X-ray patterns have minimum spacings of about 34°. The normal pattern, d = 171 Å, is shown in Fig. 2 *A* and the swollen pattern, d = 247 Å, is shown in Fig. 2 *B*. The diffraction pattern of the same swollen nerve after placing in Ringer's solution for several hours is shown in Fig. 2 *C*. The diffraction patterns in Figs. 2 *A* and 2 *C* are very similar. They have the same repeat distance, d = 171 Å, and the intensities of the first five orders are almost identical. Thus, the swelling process is reversible in that the structure of the myelin layers is the same, before and after swelling in glycerol solutions. Small differences are detected in that the reflections in Fig. 2 *C* are slightly broader than those in the normal pattern. The broadening indicates that the ordering of the myelin layers is not as precise as before swelling but the molecular structure of the myelin layers remains unchanged.

The low-angle X-ray data from frog sciatic nerve swollen in 6.5% glycerol solutions are plotted in Fig. 3 while data from nerve swollen in 0, 15, and 50% glycero

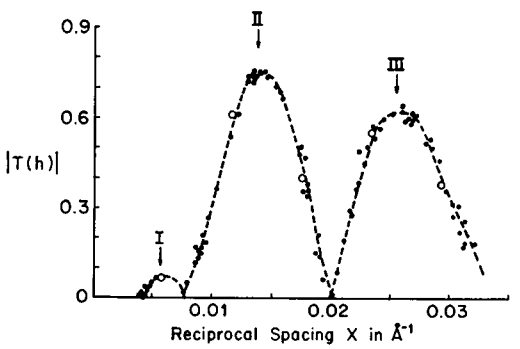

FIGURE 3 Low-angle X-ray diffraction data from normal nerve myelin in Ringer's solution (d = 171 Å) and nerve myelin swollen in 6.5% glycerol (d = 190–260 Å). The Fourier transform values $|T(h/d)|$ are plotted versus reciprocal space coordinate X. The Fourier transform values of normal nerve are indicated by open circles (○), while the Fourier transform values of swollen nerve are indicated by small black dots (●). The continuous transform (dotted line) has been drawn in by eye, and regions I, II, and III of the transform are indicated.

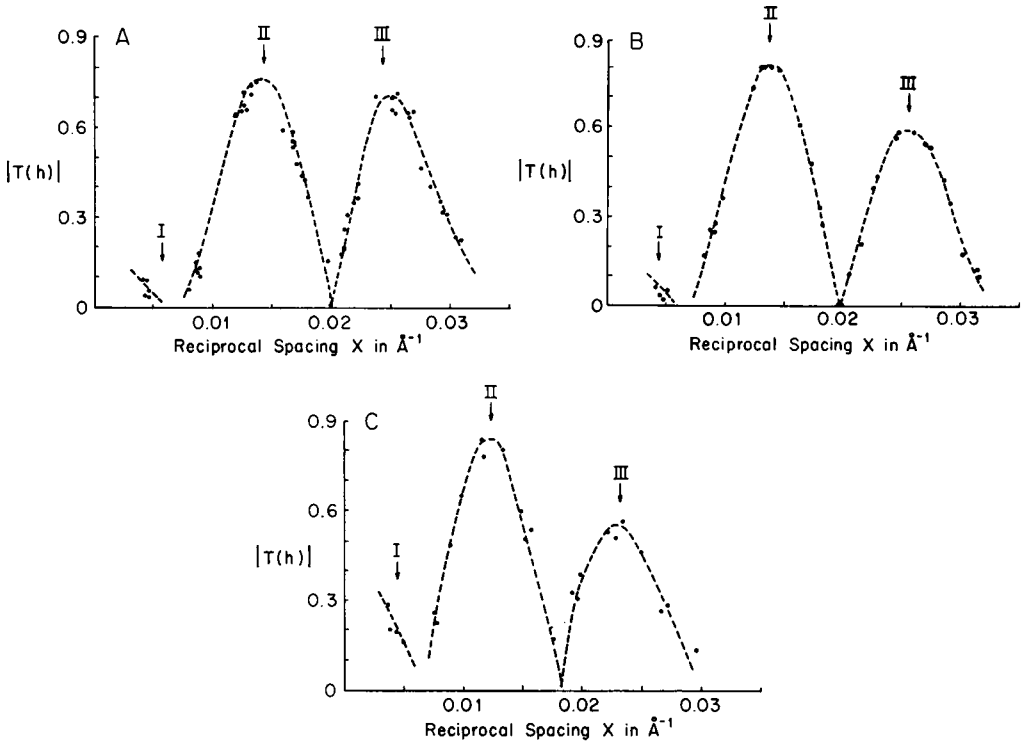

FIGURE 4 (*A*) Low-angle X-ray diffraction data from nerve myelin swollen in water. (*B*) Low-angle X-ray diffraction data from nerve myelin swollen in 15% glycerol. (*C*) Low-angle X-ray diffraction data from nerve myelin swollen in 50% glycerol. In *A–C*, the Fourier transform values are represented by small black dots (●) and are plotted versus reciprocal space coordinate X. The continuous transform (dotted line) has been drawn in by eye.

solutions are plotted in Figs. 4 *A*, *B*, and *C*, respectively. Experimentally, the intensity $I(h)$ is measured but the corrected intensity $J(h)$ is needed where $J(h) = |T(h)|^2$. It is convenient to use $|T(h)|$, the modulus of the Fourier transform recorded at $X = h/d$ and to plot these values against reciprocal spacings X in $Å^{-1}$. The repeat periods of the swollen patterns vary from $d = 190$ Å to $d = 270$ Å, and no attempt has been made to identify different data sets when using the same glycerol concentration. Different sets of X-ray data obtained using the same glycerol concentration have been put on the same relative scale using a formula given by Worthington and Blaurock (1969 *b*). The swollen nerve data $|T(h)|$ values are identified as small black dots in Figs. 3 and 4 and are plotted out to reciprocal spacing values of 0.30–0.35 $Å^{-1}$ (which corresponds to a minimum spacing of $\lesssim 34$ Å). In each case the swollen nerve data points trace out a continuous curve and this curve, which is shown as a dotted line, has been drawn in by eye. There are three separate peaks I, II, and III in each of the continuous curves of Figs. 3 and 4. These continuous curves are, how-

ever, not the same for, from Eq. 4, the diffracted amplitude is dependent on the fluid density.

The X-ray data for frog sciatic nerve swollen in 6.5% glycerol is of special interest as Ringer's solution and 6.5% glycerol solution have the same electron density of 0.338 electrons/Å^3. Many X-ray experiments have been conducted using nerve swollen in 6.5% glycerol in order to accurately define the Fourier transform (modulus) curve shown in Fig. 3. If the structure of the membrane pair was the same in Ringer's solution and in 6.5% glycerol, then, from Eq. 4, both the normal and swollen nerve would have the same Fourier transform. Note that Eq. 4 refers to $\Delta T(X)$ but $\Delta T(h) = T(h)$ when the $h = 0$ reflection is not observed. The $|T(h)|$ data points for frog sciatic nerve in Ringer's solution are identified as large open circles and are plotted in Fig. 3 together with the data points from nerve swollen in 6.5% glycerol. It is seen that the X-ray data from normal nerve fit very nicely on the Fourier transform of the nerve swollen in 6.5% glycerol. Thus, the molecular structure of the membrane pair is the same for both the normal nerve and nerve swollen in 6.5% glycerol.

INTERPRETATION

The continuous curves in Figs. 3 and 4 define three separate regions in the Fourier transform which are referred to as regions I, II, and III. Each region can be $\{\pm\}$ and there are 2^3 possible phase choices. Note that if the normal pattern is considered separate from the swelling data, then there are $2^5 = 32$ possible phase choices for live nerve. But, from Fig. 3, live nerve has the same Fourier transform as nerve swollen in 6.5% glycerol and hence there are only eight phase choices to consider. The normal nerve pattern has the $h = 1$ order in region I, the $h = 2,3$ orders in region II, and the $h = 4,5$ orders are in region III. In order to obtain the structure of both normal and swollen nerve, the phases of regions I, II, and III are required. The structure analyses (to be described) refer specifically to the normal nerve data and to the 6.5% glycerol swollen nerve data shown in Fig. 3. However, the same kinds of analyses also apply to the swollen nerve data in Figs. 4 *A*, *B*, and *C*.

The direct methods of structure analysis refer to the deconvolution and reconstruction methods. These direct methods when applied to the swelling data of nerve give the correct phases but there is a $(\pm)$ ambiguity. That is, the deconvolution and reconstruction methods can in theory reduce the phase possibilities to two choices: the correct phase choice which corresponds to $+\Delta t(x)$ and the exact opposite phase choice which corresponds to $-\Delta t(x)$. After the two choices have been obtained, the ambiguity between $+\Delta t(x)$ and $-\Delta t(x)$ will be resolved from a study of the swelling data recorded using different concentrations of glycerol.

DECONVOLUTION METHODS

The deconvolution method refers to a deconvolution of the autocorrelation function $\Delta A(x)$ where $\Delta A(x)$ is defined by the relation

$$\Delta A(x) = \Delta t(x) * \Delta t(-x), \tag{5}$$

and where * is the convolution symbol. The autocorrelation function is obtained from a Fourier transformation of the continuous intensity transform, that is, $\Delta A(x) \rightleftarrows \Delta J(X)$. $\Delta A(x)$ can be deconvoluted to give an n-strip electron density model for $\Delta t(x)$ but two solutions $\pm\Delta t(x)$ are obtained. These two solutions refer to the positive and negative structures. Deconvolution is carried out using either the recursion or the relaxation method. The recursion method is the simplest but unfortunately this method does not work for nerve myelin. The reason for this failure is that the electron density contrast between the outer edge of $m(x)$ and the fluid medium is small and any errors in the end points tend to build up as other density values are derived (Worthington et al., 1973). The relaxation method is therefore used.

In the relaxation method an n-strip model $s(x)$ is proposed as a solution. The autocorrelation function $s(x) * s(-x)$ is calculated and compared with the observed $\Delta A(x)$ via a residual function $R(x)$ where

$$R(x) = \Delta A(x) - s(x) * s(-x). \tag{6}$$

The solution $s(x)$ is varied until $R(x)$ is minimized. A systematic procedure is used in order to examine each possible phase choice. A model $s(x)$ is first derived from the Fourier synthesis computed using the particular phase choice. The minimized residual $R(x)$ is obtained for each solution corresponding to each possible phase choice. The actual minimization was obtained by using the conjugate gradient method (Fletcher and Reeves, 1964). The ($\pm$) phase choice which gives the lowest $R(x)$ is the correct one.

Experimentally the autocorrelation function $\Delta A(x)$ can be obtained from the X-ray data presented in Fig. 3. It was originally hoped that the swelling data would have a repeat period $d \geq 2v$, where v is the membrane pair width, so that $\Delta A(x)$ could be obtained directly from the Patterson function using one set of data (Worthington et al., 1973). However, the repeat distances were in the range of $d = 190$ Å to $d = 270$ Å and, as v was likely to be about 160 Å (Worthington, 1972), another method was used. A fictitious period of $d = 360$ Å was chosen and transform values at intervals of h/d were obtained from the continuous curve in Fig. 3 and a Patterson function was computed using Eq. 3. This Patterson function is accurately identifiable with $\Delta A(x)$, the autocorrelation function, provided that the baseline of the Patterson function is shifted such that $\Delta A(v) = 0$ (Worthington et al., 1973). The actual value of v can be obtained from the Patterson function as v is the value of the radial distance x where the Patterson function levels off and is parallel to the x axis. Accordingly, a value of $v = 160$ Å was obtained.

The $\Delta A(x)$ curve is not dependent on the sampling interval as long as a period of $d > 2v$ is chosen. A period of $d = 360$ Å was used in the deconvolution analysis. However, in order to show that the Patterson function does level off and is parallel to the x axis for $x > v$ a Patterson function was calculated using a larger period of

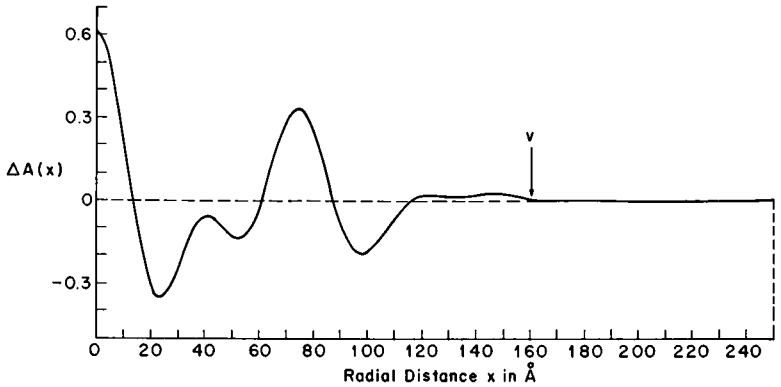

FIGURE 5 The autocorrelation function $\Delta A(x)$ for a single unit cell of nerve myelin. The membrane pair width v = 160 Å is indicated by an arrow.

d = 500 Å. $\Delta A(x)$ was then obtained by shifting the base line so that $\Delta A(160) = 0$. The autocorrelation function $\Delta A(x)$ is shown in Fig. 5, and it is seen that $\Delta A(x)$ is effectively zero for $x > 160$ Å.

The correctness of the choice of v, the membrane pair width, can be examined by computing the Fourier transform of $\Delta A(x)$ (Worthington et al., 1973). If v is correctly chosen, then

$$\Delta J(X) = 2 \int_0^v \Delta A(x) \cos 2\pi Xx \, dx. \tag{7}$$

Thus, the continuous intensity transform $\Delta J(X)$ is computed using Eq. 7 with v = 160 Å. The calculated intensity curve $\Delta J(X)$ together with the 6.5% glycerol swelling data points $J(h)$ are shown in Fig. 6. It is seen that the experimental data points fit very close to the theoretical curve and hence the chosen value of v = 160 Å is quite accurate. Note that the choice of v = 160 Å means that live nerve has an extracellular fluid layer $d - v \approx 11$ Å.

The deconvolution of $\Delta A(x)$ was carried out using a uniform strip model; the strips were 4 Å wide and v = 160 Å. The residual function $R(x)$ from Eq. 6 is expressed in terms of an agreement index AI where

$$\text{AI} = \frac{\Sigma \mid R(x) \mid}{\Sigma \mid \Delta A(x) \mid} (100\%). \tag{8}$$

The AI values for the eight phase choices are listed in Table I. The phase choices $(-, +, -)$ and $(+, -, +)$ for regions I, II, and III have the lowest AI value and are therefore the correct choices. Note that, because of the $(\pm)$ ambiguity, these two choices cannot be distinguished by the deconvolution method.

The above conclusion that the lowest AI value corresponds to the correct structure assumes that the differences in the AI values in Table I are real. The experimental

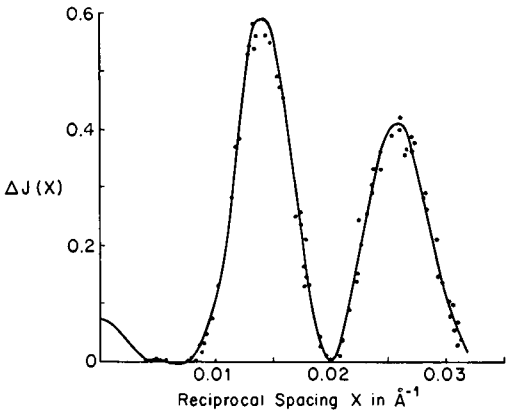

FIGURE 6 The continuous intensity curve $\Delta J(X)$ plotted versus reciprocal space coordinate X. The theoretical curve (solid line) was computed from Eq. 7 with v = 160 Å. The experimental intensities are represented by small black dots (●).

TABLE I

AGREEMENT INDEX (AI) VALUES* FOR THE EIGHT PHASE CHOICES OF THE FOURIER TRANSFORM

Phases			AI values
Region: I	II	III	
			%
−	+	−	4.1
+	−	+	
+	+	−	5.6
−	−	+	
−	+	+	7.4
+	−	−	
+	+	+	7.6
−	−	−	

* An AI value of 0.6% corresponds to the estimated error in intensity measurement.

error in intensity measurement is estimated to be 4%. This intensity error corresponds to an AI value of 0.6% and therefore this error is small compared with differences in the AI values. It might be expected that the correct phase choice would have an AI value equal to the experimental error of 0.6%. But, because $A(x)$ has a finite number of strips and because $\Delta A(x)$ has limited resolution, the AI values approach a minimum limiting value of about 4%. This limiting value is independent of the

actual phase choice for the same computational procedures are used for each of the eight phase choices.

Various studies were made in order to verify that the differences in the AI values in Table I are real. The finite size of the magnitude of this limiting AI value was verified by running a trial problem. $A(x)$ was calculated from a specified electron density strip model. The AI values associated with the various phases were then obtained by the relaxation method. This test system with no experimental error involved had an AI value of about 3% for the correct phase choice. It was also verified that the minima in $R(x)$ are the true minima. This was done by rerunning the relaxation method using different sets of data obtained from Fig. 3. For each set of data the phase choices $(-, +, -)$ and $(+, -, +)$ gave the lowest AI values and the results of the deconvolution were very similar to those of Table I. The actual choice of v should also be discussed. Although v must be determined accurately for the recursion method of deconvolution to function correctly, the exact value of v is not of critical importance in the relaxation method (Worthington et al., 1973). This has been verified by carrying out a deconvolution of $A(x)$ using both $v = 155$ Å and $v = 165$ Å, and again, the phase choices $(-, +, -)$ and $(+, -, +)$ gave the lowest AI values in each case.

From the above considerations, it follows that the differences in AI values in Table I are real. Thus, the deconvolution method clearly indicates that the phases of regions I, II, and III are either $(-, +, -)$ or $(+, -, +)$.

RECONSTRUCTION METHODS

The continuous transform (modulus) $|T(X)|$ curve in Fig. 3 is consistent with only two phase choices, the correct choice and the exactly opposite set of phases. These choices $\pm\Delta t(x)$ can be found by either computing Fourier syntheses using Eq. 2 for all phase possibilities or by computing the sampling theorem series expressions for the continuous transform $\Delta T(X)$ and using all phase choices. These methods require at least two sets of X-ray data $J(h)$ and $J(H)$ which have repeat periods d and D and which lie on the same intensity transform $J(X)$. The various sets of X-ray data from nerve swollen in 6.5% glycerol and the X-ray data from normal nerve all satisfy these criteria.

Sampling Theorem Methods

The appropriate expression for a reconstruction of $\Delta T(X)$ is

$$\Delta T(X) \approx \sum_{-h}^{h} \{\pm\} |\Delta T(h)| \operatorname{sinc}(\pi dX - \pi h). \tag{9}$$

A finite number of orders (h) are used in the summation and the reconstruction of $\Delta T(X)$ therefore only refers to the observed diffraction range. The expression in Eq. 9 contains the $\Delta T(0)$ term which is not recorded experimentally.

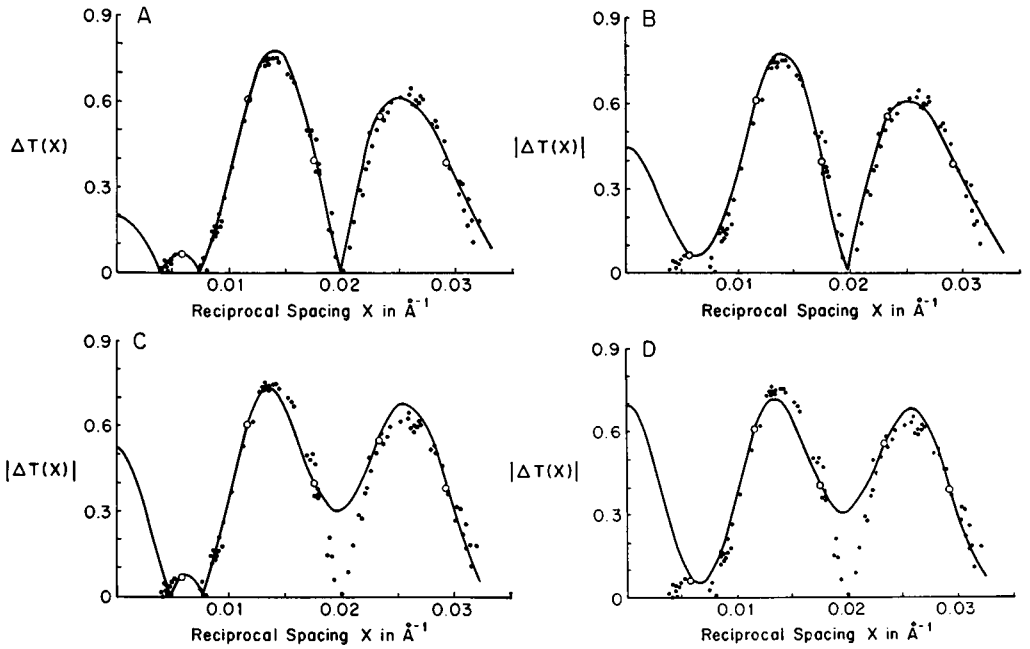

FIGURE 7 (*A*) The modulus of the continuous transform $|\Delta T(X)|$ plotted versus reciprocal space coordinate X. The $|\Delta T(X)|$ curve (solid line) was computed using the sampling theorem and normal data, $d = 171$ Å, with phases $(-, +, -)$ or $(+, -, +)$ for regions I, II, and III. In *A–D*, the Fourier transform values of normal myelin are indicated by open circles (○), while the corresponding values for myelin swollen in 6.5% glycerol are indicated by small black dots (●). (*B*) The $|\Delta T(X)|$ curve (solid line) was computed using the sampling theorem and normal data, $d = 171$ Å, with phases $(+, +, -)$ or $(-, -, +)$ for regions I, II, and III. (*C*) The $|\Delta T(X)|$ curve (solid line) was computed using the sampling theorem and normal data, $d = 171$ Å, with phases $(-, +, +)$ or $(+, -, -)$ for regions I, II, and III. (*D*) The $|\Delta T(X)|$ curve (solid line) was computed using the sampling theorem and normal data, $d = 171$ Å, with phases $(+, +, +)$ or $(-, -, -)$ for regions I, II, and III.

Before $\Delta T(X)$ can be computed from Eq. 9, a value of $\Delta T(0)$ is needed for each phase choice. The following procedure is used (King and Worthington, 1971). The normal nerve data $J(h)$ and one set of the 6.5% glycerol data $J(H)$ with repeat period D are chosen. In Eq. 9 the particular values of $\Delta T(X)$ at $X = H/D$ are substituted in turn and hence H values of $\Delta T(0)$ are obtained for each phase choice. An average value is then obtained for $\Delta T(0)$ and this average value is different for each phase choice. $\Delta T(X)$ for normal nerve is then computed using Eq. 9. Note that the live nerve data lies exactly on the $\Delta T(X)$ curve as required by the computation and is independent of the phase choice. The continuous Fourier transform curves $|\Delta T(X)|$ together with the normal nerve data (open circles) and the 6.5% glycerol nerve data (small black dots) are shown in Fig. 7. The $|\Delta T(X)|$ curves together with the experimental data points for all phase possibilities in regions I, II, and III are shown in

Figs. 7 *A*, *B*, *C*, and *D*, respectively. It is seen that the experimental data points (small black dots) lie much closer to the $|\Delta T(X)|$ curve in Fig. 7 *A*, and thus either the phase choice (−, +, −) or the phase choice (+, −, +) for regions I, II, and III is likely to be correct.

Fourier Synthesis Methods

The Fourier series representation for $\Delta t(x)$ or $t(x)$ is given by Eq. 2. The procedure is to use two sets of X-ray data which lie on the same transform (Fig. 3). The normal nerve data $J(h)$, d = 171 Å and one set of the 6.5% glycerol nerve data $J(H)$,

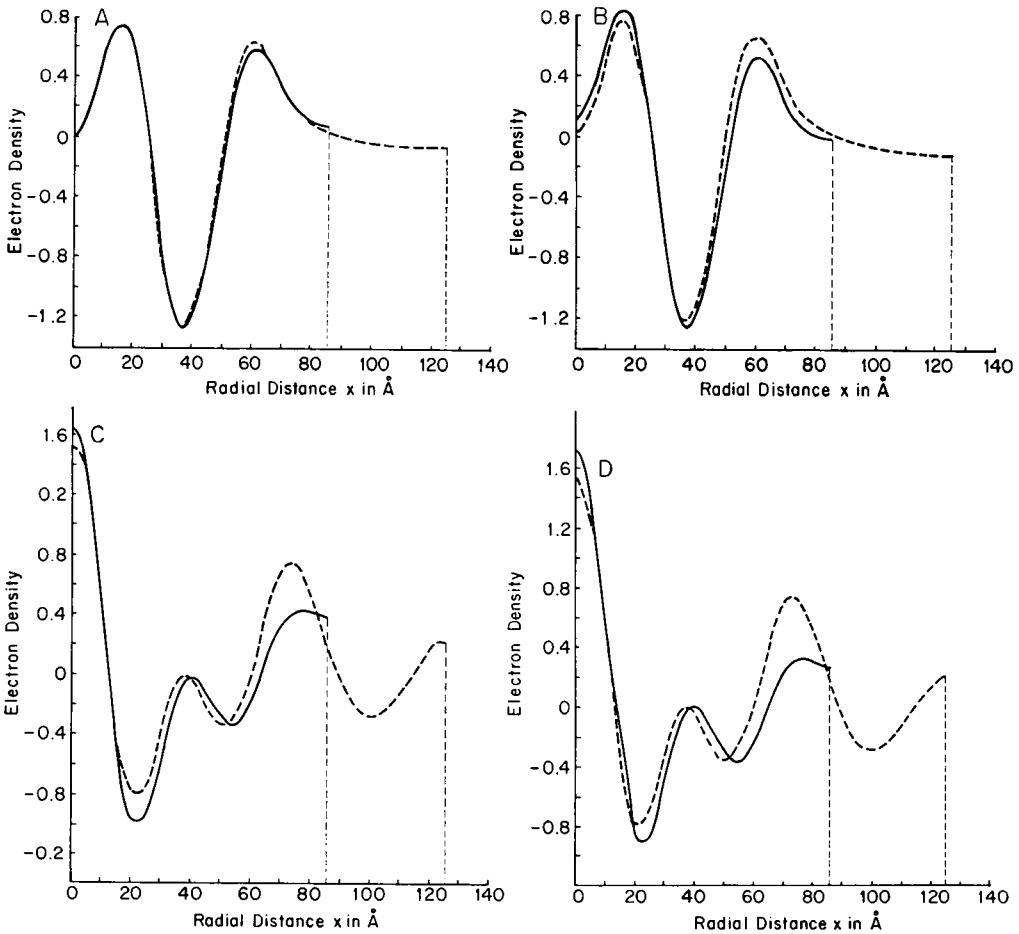

FIGURE 8 Fourier series representations for normal nerve myelin, d = 171 Å (solid line), and nerve myelin swollen in 6.5% glycerol, d = 250 Å (dotted curve); (*A*) for phase choice (−, +, −) for regions I, II, and III; (*B*) for phase choice (+, +, −) for regions I, II, and III; (*C*) for phase choice (−, +, +) for regions I, II, and III; (*D*) for phase choice (+, +, +) for regions I, II, and III.

D = 250 Å are chosen. Fourier syntheses are computed for normal and swollen nerve using phase choices (−, +, −), (+, +, −), (−, +, +), and (+, +, +) for regions I, II, and III and are shown in Figs. 8 *A*, *B*, *C*, and *D*, respectively. Note that the exact opposite phase choices would give these same profiles, except inverted. The Fourier profiles of normal and swollen nerve in Fig. 8 *A* are almost identical for radial distances x = 0 to x = 80 Å whereas the Fourier profiles of normal and swollen nerve are markedly different in Figs. 8 *B*, *C*, and *D*. Hence the Fourier comparisons indicate that the phase choices (−, +, −) and (+, −, +) in regions I, II, and III are likely to be correct.

Note that the Fourier synthesis and the sampling theorem methods are essentially equivalent as they are related to each other via a Fourier transformation (Worthington et al., 1973). The Fourier method is more straightforward in that the h = 0 reflection is not used. Although the two methods are essentially equivalent, it is, nevertheless, instructive to use both methods and the Figs. 7 and 8 clearly demonstrate the correctness of either the phase choice (−, +, −) or the phase choice (+, −, +) for regions I, II, and III of the Fourier transform.

CHOICE BETWEEN THE POSITIVE AND NEGATIVE STRUCTURE

The choice between the positive and negative structures for nerve myelin has already been made in an earlier study (McIntosh and Worthington, 1973). The positive structure was defined as the structure corresponding to the phase choice (−, +, −) and the negative structure therefore corresponded to the exactly opposite phase choice (+, −, +). Swelling experiments were carried out using two different fluids, 0% glycerol (0.334 electrons/Å^3) and 20% glycerol (0.346 electrons/Å^3). Fourier syntheses computed using the phase choice (−, +, −) for regions I, II, and III and these two sets of data reconstructed these different fluid levels. The electron density level for the 20% glycerol fluid layer was above the electron density level for the 0% glycerol fluid layer. If Fourier syntheses are computed using (+, −, +) phases corresponding to the negative structure, then these fluid electron density levels are reversed and this is clearly impossible. Thus, the positive structure for live nerve which has phases (−, +, +, −, −) for the h = 5 orders is correct.

This study has been repeated on many occasions. In order to further demonstrate the correctness of the positive structure, two sets of swelling data using 6.5% glycerol, d = 226 Å and 20% glycerol, d = 214 Å are chosen. The Fourier syntheses are computed using the phase choice corresponding to the favored positive structure and are shown in Fig. 9. The electron density level of the 20% glycerol fluid layer is higher than the electron density level of the 6.5% glycerol fluid layer. On the other hand, if Fourier syntheses are computed using the phases corresponding to the negative structure, then the profiles in Fig. 9 are inverted so that these fluid levels are

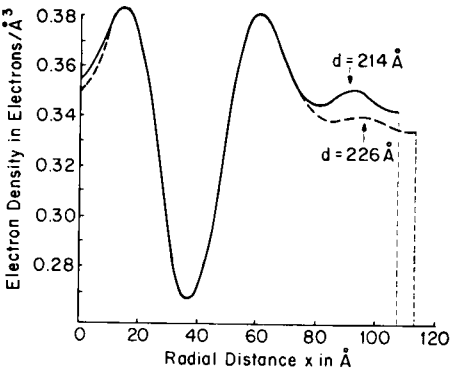

FIGURE 9

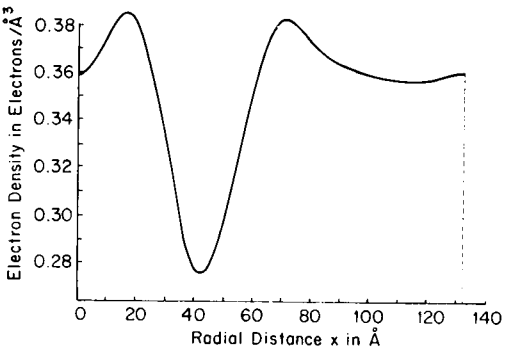

FIGURE 10

FIGURE 9 Fourier series representations for nerve myelin swollen in 20% glycerol, d = 214 Å (solid curve), and nerve myelin swollen in 6.5% glycerol, d = 226 Å (dotted curve), for phase choice (−, +, −) for regions I, II, and III. An absolute electron density scale for these syntheses is included.

FIGURE 10 Fourier series representation on an absolute electron density scale for nerve myelin swollen in 50% glycerol, d = 263 Å, phase choice (−, +, −) for regions I, II, and III.

reversed and this is incorrect. Hence it can be concluded that the positive structure for live nerve with phases (−, +, +, −, −) for the h = 5 orders is the correct choice.

ELECTRON DENSITY SCALE IN ELECTRONS/Å³

An electron density scale in electrons/Å³ for nerve myelin was first derived by evaluating M, the average electron density of the membrane pair, and from knowledge of F, the electron density of the fluid medium (Worthington and Blaurock, 1969 *b*). Fourier profiles of nerve myelin at low resolution have been shown with an electron density scale superimposed (Worthington, 1973 *a*). An electron scale can be readily assigned to the Fouriers of normal nerve and nerve swollen in glycerol solutions. Consider two sets of swelling data using 6.5% glycerol, d = 226 Å and 20% glycerol, d = 214 Å. The Fourier syntheses are shown in Fig. 9. The fluid layer of 20% glycerol has an electron density of 0.346 electrons/Å³ and the fluid layer of 6.5% glycerol has an electron density of 0.338 electrons/Å³. The electron density profile of the individual membranes superimpose almost exactly but the fluid layers are at different levels. Assignment of the electron densities to these levels provides an electron density scale and this scale in electrons/Å³ is shown in Fig. 9. The electron density levels of the nerve membrane profile in Fig. 9 agree closely with the earlier electron density levels for nerve myelin (Worthington and Blaurock, 1969 *b*). The electron density scale derived here is also consistent with the swelling data using glycerol solutions; the data is shown in Fig. 3 and Figs. 4 *A*, *B*, and *C*.

FOURIER PROFILES OF NORMAL AND SWOLLEN NERVE

It has been demonstrated that the electron density profiles of normal nerve and nerve swollen in 6.5% glycerol are identical. These profiles are shown in Fig. 8 *A* and the 6.5% glycerol nerve profile in Fig. 9 has an electron density scale superimposed. From Fig. 9 the nerve swollen in 20% glycerol has a profile very similar to the profile shown by the nerve swollen in 6.5% glycerol. In summary, it can be demonstrated by computing Fourier syntheses of normal and swollen nerve that the electron density profile of the nerve myelin membrane is the same in Ringer's solution and in glycerol solutions which have a concentration range of 0–20%.

There is evidence from Fig. 9 that glycerol at a concentration of 20% is transported from the extracellular side to the cytoplasmic side of the membrane. However, according to the Fourier profiles, the glycerol solutions do not remain within the individual membranes, or, at least, do not remain in sufficient quantities to be detected by X-ray diffraction. On the other hand, when glycerol concentrations above 20% are used to obtain swelling, changes in the nerve membrane profile have been noticed. These changes become more noticeable with increase in concentration. A Fourier synthesis was computed using one set of data obtained from nerve swollen in 50% glycerol, $d = 263$ Å and is shown in Fig. 10. An electron density scale in electrons per cubic angstrom is superimposed in Fig. 10. Comparison of this Fourier profile with the Fourier profiles in Fig. 8 shows that the individual membrane of the nerve in 50% glycerol is a little wider and the low density region is also wider and has a slightly higher electron density level. The nerve in 50% glycerol has a higher density at $x = 0$ (Fig. 10) compared with densities at $x = 0$ of nerve in lower glycerol concentrations (Fig. 9). This implies that glycerol has been transported from the extracellular side into the cytoplasmic region between the individual membranes of the membrane pair. Thus, at glycerol concentrations above 20%, sufficient quantities of glycerol remain in the nerve myelin membrane to be detected by X-ray diffraction.

This change in the nerve membrane profile brought about by swelling has been noted previously in the case of nerve swollen in sucrose solutions (Worthington and Blaurock, 1969 *b*). The width of the low density region showed increases with sucrose concentrations as low as 5%. The photoreceptor membranes have also been studied by X-ray diffraction after treatment with glycerol solutions (Worthington, 1973 *b*). In this case, changes in the membrane profile are noticeable with glycerol concentrations as low as 5%. However, in the present study, the nerve membrane profile remains unchanged when nerve is swollen in glycerol solutions with concentrations ranging from 0% to as high as 20%. This finding is in keeping with the idea that the nerve myelin membrane is relatively impermeable as it functions as an insulator during nerve conduction.

EXPERIMENTAL VERIFICATION OF THE PHASE CHOICE

The phase choice $(-, +, +, -, -)$ for the $h = 5$ orders of live nerve has been shown to be correct by using deconvolution and reconstruction methods and from a study of the swelling data recorded using different glycerol concentrations. If, for argument's sake, the favored phase choice was considered uncertain, then the second choice $(+, +, +, -, -)$ would become a possibility. In earlier work (Worthington and Blaurock, 1969 *b*) the phase of the $h = 1$ order was the most difficult to assign as region I had the smallest intensity. The phase of region I can be studied experimentally.

A series of X-ray experiments was carried out with glycerol added to Ringer's solution. The idea is that the salt ions in the Ringer's solution will prevent swelling but the glycerol will change the electron density of the fluid layer in nerve. The glycerol will diffuse into the extracellular fluid layer of nerve for this layer is about 11 Å for normal nerve whereas the glycerol molecule is about 6 to 7 Å in diameter. Thus, the electron density of the extracellular fluid layer can be varied without any increase in the repeat period.

Two sets of X-ray data $\Delta T_1(h)$ and $\Delta T_2(h)$ obtained using two different immersion fluids F_1 and F_2 and which have the same period d are compared. From Eq. 4, $\Delta T_2(h)$ can be expressed in terms of $\Delta T_1(h)$ where

$$\Delta T_2(h) = \Delta T_1(h) - (F_2 - F_1)\, v \operatorname{sinc} \pi v h/d. \tag{10}$$

Let F_1 refer to Ringer's solution (0.338 electrons/Å^3) and F_2 refer to 5% glycerol in Ringer's solution (0.341 electrons/Å^3). The membrane pair width v is 160 Å. The transform changes due to increasing the fluid density in a relatively small step of 0.003 electrons/Å^3 are given by Eq. 10. Relative to normal nerve in fluid F_1 the intensities $J_2(h)$ of nerve in a denser medium F_2 change in the following manner. The first-order intensity $J_2(1)$ will increase, if the $h = 1$ phase of normal nerve is $(-)$. The $J_2(2)$ intensity will increase, if the $h = 2$ phase is $(+)$ while the $J_2(3)$ intensity will decrease, if the $h = 3$ phase is $(+)$. The intensities of the $h = 4,5$ orders are insensitive or only weakly influenced by these fluid changes for the sinc $\pi v h/d$ term in Eq. 10 falls off rapidly with increase in h. The crucial intensity change is that of $J_2(1)$ for if the $h = 1$ phase is $(-)$, then $J_2(1)$ increases relative to normal nerve whereas if the $h = 1$ phase is $(+)$, then $J_2(1)$ decreases relative to normal nerve.

Typical diffraction patterns of frog sciatic nerve in glycerol and Ringer's solution are shown in Fig. 11. All three X-ray patterns show $d = 171$ Å with $h = 5$ orders and have minimum spacings of 34 Å. The normal pattern of frog sciatic nerve in Ringer's solution is shown in Fig. 11 *A*. The patterns obtained from frog sciatic nerve with 5% and 10% glycerol solutions added to the Ringer's solution are shown in Figs. 11 *B* and *C*, respectively. The fluids used to obtain the X-ray patterns shown in Figs. 11 *A*, *B*, and *C* are 0, 5, and 10% glycerol in Ringer's solution and have electron densities 0.338, 0.341, and 0.344 electrons/Å^3, respectively. The intensities of the

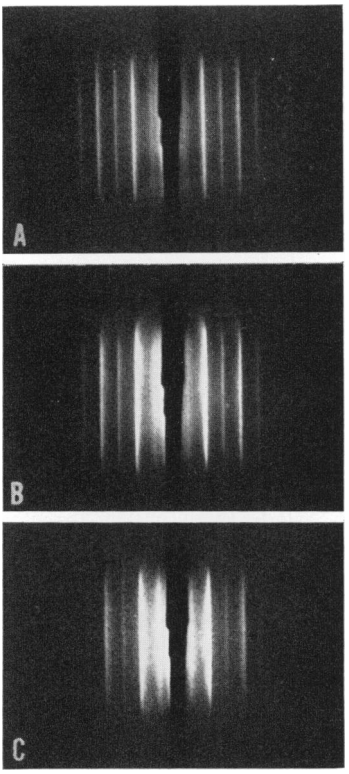

FIGURE 11 (*A*) Low-angle X-ray diffraction pattern of normal nerve myelin, d = 171 Å, in Ringer's solution. (*B*) Low-angle X-ray diffraction pattern of nerve myelin, d = 171 Å, in Ringer's solution with 5% glycerol added. Note that the first and second orders of diffraction are more intense for the pattern of Fig. 11 *B* than for the pattern of Fig. 11 *A*. (*C*) Low-angle X-ray diffraction pattern of nerve myelin, d = 171 Å, in Ringer's solution with 10% glycerol added. The first and second orders of diffraction are more intense for the pattern of Fig. 11 *C* than for the patterns of Fig. 11 *B* or Fig. 11 *A*. Note that the intensity of the third order of diffraction decreases from Fig. 11 *A* to *B* to *C*.

X-ray pattern in Fig. 11 *B* relative to the normal nerve pattern show increases in the $h = 1,2$ orders and a decrease in the $h = 3$ order. The intensities of the X-ray pattern in Fig. 11 *C* relative to the pattern in Fig. 11 *B* follow the same trend and show increases in the $h = 1,2$ orders and a decrease in the $h = 3$ order. Thus, it can be concluded from these experiments that $(-, +)$ is the phase choice for regions I and II. These experiments therefore provide direct verification of the correctness of the phases $(-, +, +)$ for the first three orders of live nerve.

DISCUSSION

New and extensive low-angle X-ray diffraction data have been recorded from nerve myelin swollen in glycerol solutions. The molecular structure of the membrane pair does not change on swelling provided that the glycerol concentration does not exceed

15%. The only effect of swelling nerve is to increase the width of the extracellular fluid layer. Direct methods of structure analysis have been used to uniquely find the correct structure of normal and swollen nerve at low resolution. The correct structure for normal nerve has $(-, +, +, -, -)$ phases for $h = 5$ orders.

As noted in the introduction, this set of phases was first proposed in 1963 and this phase choice is known to be consistent with the nerve membrane having a bilayer profile. In 1969 structure analysis of the sucrose swelling data also gave this phase choice but a proof of correctness was not given. Since 1969 direct methods of structure analysis as applied to nerve myelin have been formulated and the use of these methods enable a unique choice of phases (but with the $\pm$ ambiguity) to be made. A proof of correctness is implied provided that the differences in the AI values of the deconvolution method are real or provided that the Fouriers and calculated transforms show differences that are real. In the structure analysis of the glycerol swelling data the differences in AI values have been shown to be significant and similarly the differences between Fouriers and calculated transforms are significant. All of these methods indicate that either the phases $(-, +, -)$ or the phases $(+, -, +)$ are the correct phases for regions I, II, and III of the Fourier transform. A study of the swelling data using different concentrations of glycerol clearly demonstrates that the $(-, +, -)$ phases are correct. Therefore, a proof of correctness has been obtained for the phase choice $(-, +, +, -, -)$ for the $h = 5$ orders of live nerve.

An absolute electron density scale has been derived for nerve myelin. This scale is very similar to an earlier electron density scale which was first derived in 1969. From Figs. 8 *A* and 9 the membrane profile has electron density peak values of 0.384 electrons/Å^3 and 0.380 electrons/Å^3 and a minimum value of 0.267 electrons/Å^3. The membrane profile is slightly asymmetrical with the higher density peak value of 0.384 electrons/Å^3 on the cytoplasmic side of the membrane. The asymmetry of the nerve myelin membrane was first noted in 1969 (Worthington, 1969 *a*).

X-ray evidence for the existence of an extracellular fluid layer in normal nerve was first presented in 1969 (Worthington and Blaurock, 1969 *b*). In this paper detailed evidence has been presented which supports the existence of an extracellular fluid layer of about 11 Å in width in normal nerve. The comparison (Fig. 6) between $\Delta J(X)$ computed from Eq. 7 with the swelling data and also the Fourier syntheses of normal and swollen nerve (Fig. 8 *A*) both support the choice of $d - v \approx 11$ Å for normal nerve. The X-ray experiments on nerve in glycerol and Ringer's solution provide further proof that the normal nerve has an extracellular fluid layer since this space is accessible to the immersion fluid containing glycerol.

X-ray evidence for the existence of a cytoplasmic fluid layer at the center of the membrane pair in normal nerve was first presented in 1969 (Worthington, 1969 *a*). In this paper the structure of nerve myelin has been derived without any reference to the existence of this fluid layer. However, the Fourier syntheses in Fig. 9 show that the electron density at $x = 0$ is higher for nerve in 20% glycerol than it is for nerve in 6.5% glycerol. The electron density of this cytoplasmic layer is about the

same for normal nerve and nerve swollen in glycerol concentrations from 0% to 15%. However, for glycerol concentrations of 20% and higher, the electron density of the cytoplasmic space increases. This observation indicates that for these higher glycerol concentrations some glycerol has been transported from the extracellular side to the cytoplasmic side and it appears to reside in the cytoplasmic fluid layer in between the individual membranes of the membrane pair. In Fig. 10 the electron density at $x = 0$ for nerve in 50% glycerol is higher than it is for 6.5% and 20% glycerol. In summary, the present X-ray studies provide convincing evidence for the existence of the extracellular fluid layer in normal nerve and the Fourier syntheses provide evidence which supports the existence of a cytoplasmic fluid layer in nerve.

The molecular distribution of nerve myelin is not readily obtained from Fourier syntheses as noted previously (Worthington, 1972). The present Fourier profiles have a resolution of 17 Å and at this resolution it is only possible to draw elementary and fairly obvious conclusions about the molecular assembly in nerve. However, knowledge of an electron density scale provides the electron density levels of the Fourier profile of nerve myelin. It is natural to assign the protein and lipid heads to the high density regions and to assign the hydrocarbon chains of the lipid molecules to the central low density region. A more detailed assignment of molecular components awaits the correct interpretation of the higher orders of diffraction from nerve.

This work was supported by a grant from the U. S. Public Health Service.

Received for publication 12 October 1973 and in revised form 18 January 1974.

REFERENCES

AKERS, C. K., and D. F. PARSONS. 1970. *Biophys. J.* **10**:116.
BLAUROCK, A. E., and C. R. WORTHINGTON. 1966. *Biophys. J.* **6**:305.
BLAUROCK, A. E., and C. R. WORTHINGTON. 1969. *Biochim. Biophys. Acta.* **173**:419.
BOYES-WATSON, J., and M. F. PERUTZ. 1943. *Nature (Lond.).* **151**:714.
ELLIOTT, G. F., and C. R. WORTHINGTON. 1963. *J. Ultrastruct. Res.* **9**:166.
FLETCHER, R., and C. M. REEVES. 1964. *Comput. J.* **7**:149.
FINEAN, J. B. 1969. *Q. Rev. Biophys.* **2**:1.
FINEAN, J. B., and R. E. BURGE. 1963. *J. Mol. Biol.* **7**:672.
FINEAN, J. B., and P. F. MILLINGTON. 1957. *J. Biophys. Biochem. Cytol.* **3**:89.
GEREN, B. B. 1954. *Exp. Cell Res.* **7**:558.
HARKER, D. 1972. *Biophys. J.* **12**:1285.
HOSEMANN, R., and S. N. BAGCHI. 1962. Direct Analysis of Diffraction by Matter. North-Holland Publishing, Co., Amsterdam.
KING, G. I., and C. R. WORTHINGTON. 1971. *Phys. Letters.* **35A**:259.
MCINTOSH, T. J., and C. R. WORTHINGTON. 1973. *Biophys. J.* **13**:498.
MOODY, M. F. 1963. *Science (Wash. D. C.).* **142**:1173.
PERUTZ, M. F. 1954. *Proc. R. Soc. Lond. Ser. A.* **225**:264.
ROBERTSON, J. D. 1958. *J. Biophys. Biochem. Cytol.* **3**:1043.
SCHMITT, F. O., R. S. BEAR, and K. J. PALMER. 1941. *J. Cell Comp. Physiol.* **18**:31.
SHANNON, C. E. 1949. *Proc. I. R. E.* **37**:10.
WORTHINGTON, C. R. 1969 *a. Proc. Natl. Acad. Sci. U. S. A.* **63**:604.
WORTHINGTON, C. R. 1969 *b. Biophys. J.* **9**:222.
WORTHINGTON, C. R. 1970. *Biophys. J.* **10**:675.

WORTHINGTON, C. R. 1971. *In* Biophysics and Physiology of Excitable Membranes. W. J. Adelman, editor. Van Nostrand Reinhold Company, New York.
WORTHINGTON, C. R. 1972. *Ann. N. Y. Acad. Sci.* **195**:293.
WORTHINGTON, C. R. 1971 *a. Curr. Top. Bioenerg.* **5**:1.
WORTHINGTON, C. R. 1973 *b. Exp. Eye Res.* **17**.
WORTHINGTON, C. R., and A. E. BLAUROCK. 1969 *a. Biochim. Biophys. Acta.* **173**:427.
WORTHINGTON, C. R., and A. E. BLAUROCK. 1969 *b. Biophys. J.* **9**:970.
WORTHINGTON, C. R., G. I. KING, and T. J. MCINTOSH. 1973. *Biophys. J.* **13**:480.
WORTHINGTON, C. R., and S. C. LIU. 1973. *Arch. Biochem. Biophys.* **157**:573.
WORTHINGTON, C. R., and T. J. MCINTOSH. 1973. *Nat. New Biol.* **245**:97.